# Assessment of the influence of temperature and pressure on the prediction of the precipitation of minerals during the desalination process

Barbara Tomaszewska[a,b,*], Magdalena Tyszer[b]

[a] Mineral and Energy Economy Research Institute, Polish Academy of Sciences, Wybickiego 7, 31-261 Kraków, Poland
[b] AGH - University of Science and Technology, Faculty of Geology, Geophysics and Environmental Protection, Mickiewicza 30 Av., 30-059 Kraków, Poland

## ARTICLE INFO

## ABSTRACT

The results of research designed to examine the influence of the temperature of geothermal water and trans-membrane pressure on the precipitation of selected minerals during the desalination process are presented. The geothermal water used in tests was characterised by a high conductivity value, high total hardness and elevated concentrations of sulphates, silicates, calcium, magnesium, and macro and micronutrients, which can cause scaling phenomena to occur. Based on the physicochemical composition of the water, an estimate was made of the extent of the scaling phenomena for all the processes examined. For these analyses, two parameters of the desalination process: 1) the temperature of feed water (T) and 2) the transmembrane pressure (p) were chosen and tested in different value ranges. The research results demonstrate the existence of reactions determined both by hydrogeochemical modelling and from the results obtained during real laboratory tests. It was found that in the case of carbonate (aragonite and calcite) and all silicate minerals, an increase in the pressure value to 40 bar slightly decreases the *Saturation Index* for each mineral. A reverse relationship was reported with gypsum. Increasing transmembrane pressure to 40 bar increases the tendency of the mineral form studied to precipitate.

## 1. Introduction

In recent years, the desalination of geothermal water using membrane processes has been considered as one of the potential solutions for water reuse [1–3]. However, due to the low solubility of hardness salts and depending on the process parameters used in membrane separation systems, secondary minerals may precipitate from treated water on the membrane surface [4–5]. Various operating conditions such as pH, temperature, transmembrane pressure, permeation rate, flow velocity, and the presence of other salts or metal ions can have an influence on scale formation. Crystallization or precipitation of carbonate, silicate, sulphate or other minerals can occur if the activity of specific ions in solution is above their saturation level (supersaturated) [5–7]. Some precipitation may continue to occur during processes (including membrane processes), unless the precipitation is chemically prevented. The available surface area in the membrane process can enhance the precipitation of calcium carbonate solids and cause a decline in permeate flux [8]. Supersaturation conditions can be considered as a driving force for initiating crystallization of silicate, carbonate and sulphate minerals [9]. Use of the nanofiltration (NF) process as a pre-treatment for desalination processes can potentially be a promising solution [10–12]. Kaya et al. [10] showed, on the basis of a mini,

pilot-scale membrane desalination system in Urla, that the use of a NF process as pre-treatment for desalination can contribute to such benefits as 1) reducing the scaling phenomenon in further processes (e.g. reverse osmosis) and 2) reducing the cost of the desalination process. However, input parameters such as the pressure and temperature of raw geothermal water may determine the intensity of the scaling phenomena which can exist on the surface of the nanofiltration membrane and directly impact on the efficiency of the process [10,13]. Geothermal water often exhibits high concentrations of silica, sulphates, calcium, magnesium and carbonate which can precipitate on the membrane surface and disturb the effectiveness of the process [14]. Previous research has shown that calcite, dolomite and aragonite scaling is widely encountered during the desalination of geothermal waters using membrane processes [6,14]. The degree of the scaling phenomenon observed primarily depends on the level of calcium hardness and bicarbonate alkalinity of the feed water [15–17].

There are many methods used in predicting the degree of scaling. The most popular methods are equation methods, based on the Langelier Saturation Index, Ryznar Stability Index, Pucorius Scaling Index or other measures [18]. Relative saturation indexes (%) with respect to the main salts ex.: $CaCO_3$, $CaSO_4$, $BaSO_4$, $SiO2$ are also calculated using related software. In most cases the use of numerical

---

* Corresponding author at: Mineral and Energy Economy Research Institute, Polish Academy of Sciences, Wybickiego 7, 31-261 Kraków, Poland.
*E-mail addresses:* b.tomaszewska@meeri.pl, barbara.tomaszewska@agh.edu.pl (B. Tomaszewska).

**Table 1**
Physicochemical characterisation of geothermal water tested.

| Parameters | Raw geothermal water average value [mg/L] |
|---|---|
| TH[a] | 584.5 |
| $Na^+$ | 445.42 |
| $K^+$ | 41.29 |
| $Ca^{+2}$ | 173.86 |
| $Mg^{+2}$ | 36.63 |
| $Sr^{+2}$ | 5.61 |
| $Cl^-$ | 446.70 |
| $SO_4^{-2}$ | 723.80 |
| $HCO_3^-$ | 287.70 |
| $H_2SiO_3$ | 69.90 |
| $Al^{+3}$ | 0.033 |
| $Fe^{+2}$ | 0.140 |
| $PO_4^{-3}$ | 0.526 |
| $Ba^{+2}$ | 0.0172 |
| B | 8.00 |
| EC[b] | 3.05 |
| [mS/cm] | |
| pH[c] | 6.79 |

[a] Total hardness in mg $CaCO_3$/L.
[b] Electrical conductivity in mS/cm.
[c] pH [−].

modelling permits more accurate forecasting of the precipitation phenomena. However, it depends on the range of minerals database included in the calculation and the possibility of process parameters (pressure and temperature) being incorporated in the calculations and, also, on the physicochemical properties of the feed water.

The aim of this work is to present the results of research designed to examine the influence of selected parameters such as transmembrane pressure and the temperature of feed water on the tendency to precipitate secondary minerals during the desalination process. A calculation was done using PHREEQC, a computer program for speciation, batch-reaction, one-dimensional transport, and inverse geochemical calculations [19] which is the most popular tool recommended by USGS (United States Geological Survey) and is designed to perform a wide variety of aqueous geochemical calculations. The research included all steps of analysis, from laboratory tests of selected geothermal waters, modelling research and microscopic analysis of the sediments formed on the NF membrane during the treatment processes. The purpose of the assay was to examine whether there is a reaction between process parameters (pressure, temperature) and the actual tendency to precipitate of the minerals analysed (evaluated by the variation in permeate flux).
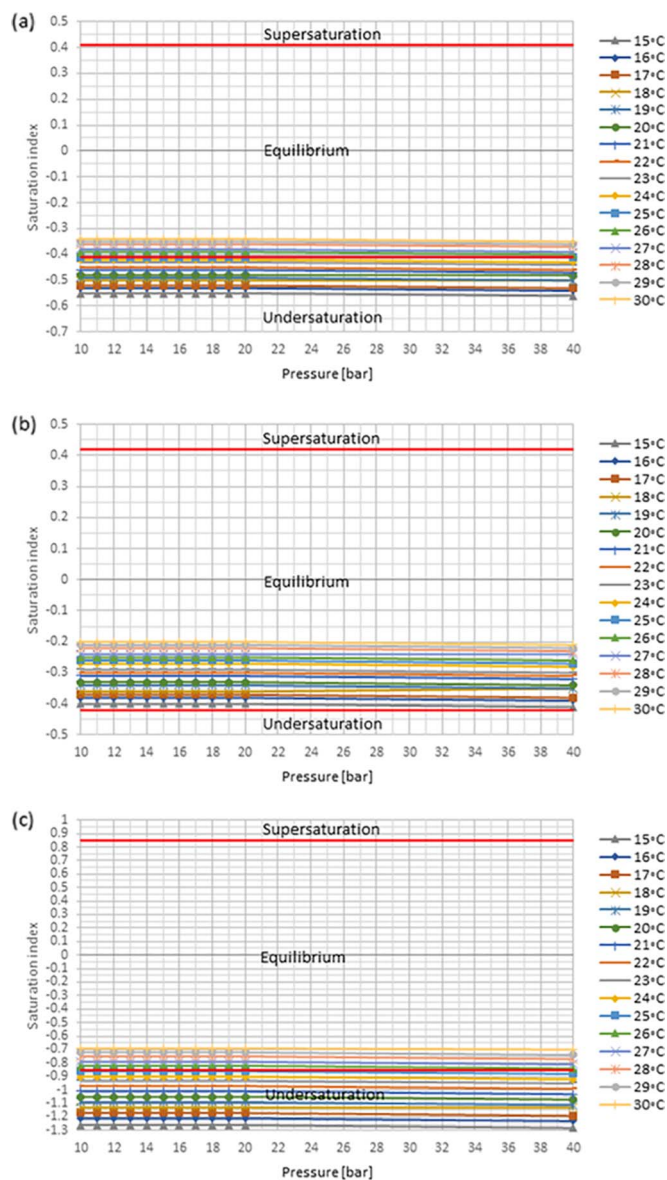


**Fig. 1.** The values of the Saturation Index for the (a) aragonite, (b) calcite and (c) dolomite solid phase in selected ranges of transmembrane pressure values (10–20 bar and 40 bar), including the value of water temperature (from 15 to 30 °C).

**Table 2**
Thermodynamic data (based on [20]).

| Species | Reaction | $H_r^o \pm 1F$ (kcal/mol) | Log $K_r^o \pm 1F$ |
|---|---|---|---|
| Aragonite | $CaCO_3 = Ca^{2+} + CO_3^{2-}$ | $-2.589 \pm 0.3$ | $-8.336 \pm 0.02$ |
| | log Kr = $-171.9773 - 0.077993\,T + 2903.293/T + 71.595\,Log_{10}T$ | | |
| Calcite | $CaCO_3 = Ca^{2+} + CO_3^{2-}$ | $-2.297 \pm 0.3$ | $-8.48 \pm 0.02$ |
| | log Kr = $-171.9065 - 0.077993\,T + 2839.319/T + 71.595\,Log10T$ | | |
| Dolomite | $CaMg(CO_3)_2 = Ca^{2+} + Mg^{2+} + 2CO_3^{2-}$ | $-11.09$ | $-16.54$ |
| Chalcedony | $SiO_2 + 2H_2O = H_4SiO_4$ | 4.72 | $-3.55$ |
| | log Kr = $-0.09 - 1032/T$ | | |
| Quartz | $SiO_2 + 2H_2O = H_4SiO_4$ | 5.99 | $-3.98$ |
| | log Kr = $0.41 - 1309/T$ | | |
| Silicagel | $SiO_2 + 2H_2O = H_4SiO_4$ | 4.44 | $-3.018$ |
| Amorphous $SiO_2$ | $SiO_2 + 2H_2O = H_4SiO_4$ | 3.34 | $-2.71$ |
| | log Kr = $-0.26 - 731/T$ | | |

$H_r^o$ – enthalpy of reaction; Log $K_r^o$ – equilibrium constant for the reaction ($K_r$-constant reaction); kcal/mol – kilocalories per mole; 1F – the uncertainty in the listed value.

**Fig. 2.** The values of the Saturation Index for (a) chalcedony, (b) quartz, (c) silica-gel and (d) amorphous $SiO_2$ solid phase in selected ranges of transmembrane pressure values (10–20 bar and 40 bar), including the value of water temperature (from 15 to 30 °C).
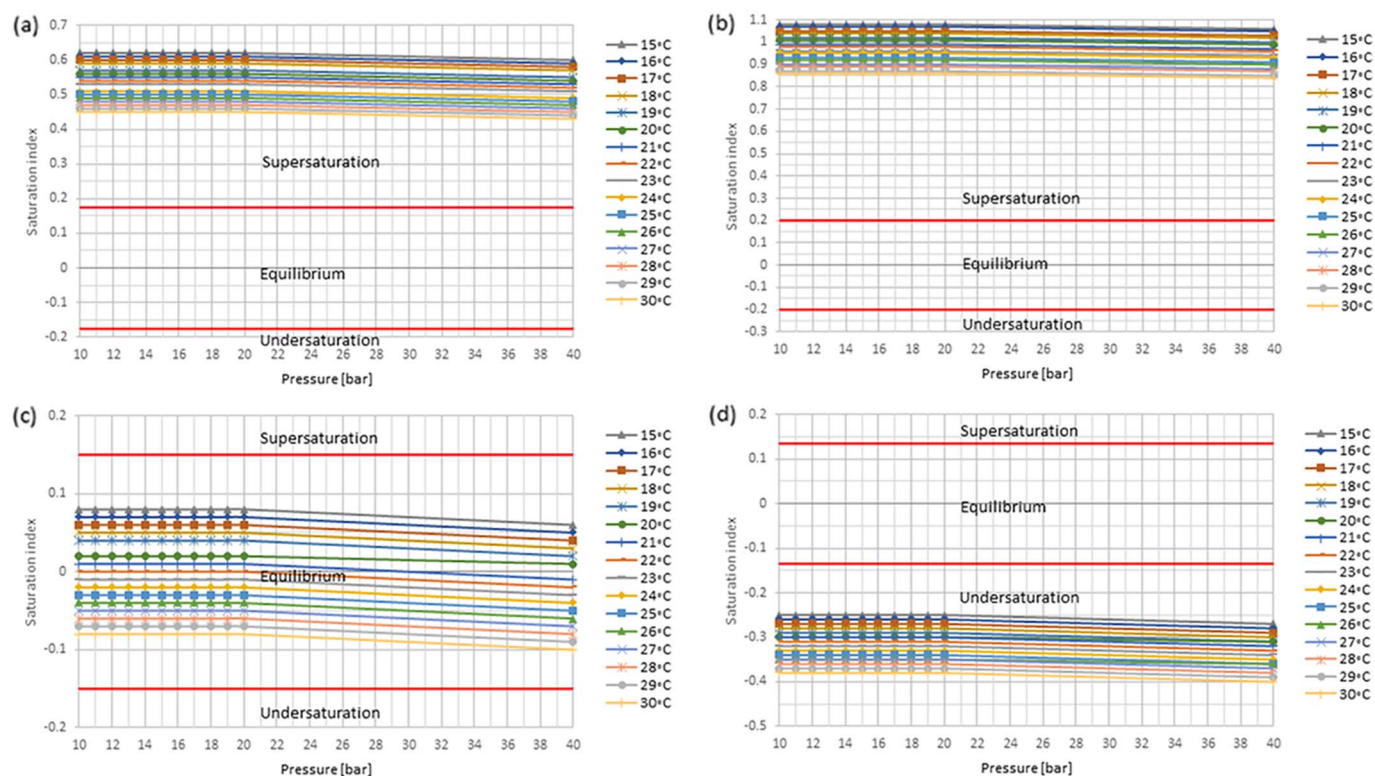
## 2. Materials and methods

### 2.1. Geothermal water

The geothermal water selected is characterised by a high conductivity value (about 3.0 mS/cm), high levels of total hardness (about 585 mgCaCO₃/L) and elevated concentrations of metasilicic acid (about 70 mg/L), sulphates (724 mg/L), calcium (174 mg/L), magnesium (37 mg/L) and other macro and micronutrients. The physical and chemical composition of the water chosen is shown in Table 1.

### 2.2. Hydrogeochemical modelling

The analyses, involving the estimation of the scaling prognosis, were conducted using the hydrogeochemical modelling program PHREEQC (*Phreeqc Interactive 3.3.3-10424* - PHREEQCI equipped with the Wateq4f minerals database [19]). In order to evaluate the scaling phenomenon, the physicochemical composition values of raw geothermal water (shown in Table 1) were used as input parameters to the SOLUTION_SPECIES in the PHREEQC program. This option defines the association reaction (chemical reaction, log K - equilibrium constant for the reaction) and the thermodynamic data (activity-coefficient parameters) for aqueous species. Additionally, the transmembrane pressure value set for the desalination process was also inputted as REACTION_PRESSURE. It specified pressure during the batch-reaction steps. The equilibrium state between water and a mineral corresponds to *SI* values ± 5% log K (*SI = 0 ± 0.05 log K*). This is because in natural conditions the phenomenon of polarisation of concentration is observed on the membrane and sediments precipitating on the membrane surface may already occur in the equilibrium state. The *SI* values above and below *0 ± 0.05 log K* refer to the states of supersaturation and undersaturation respectively. The supersaturation state indicates a

tendency of a specified mineral to precipitate from water. Table 2 shows thermodynamic data of the reaction in water, specifically the carbonate, silicate and sulphate mineral forms, in cases when a pressure reaction is not allowed.

Specific volumes of aqueous species are calculated as a function of the dielectric properties of water and the ionic strength of the solution, which allows the calculation of pressure effects on the chemical reaction and the concentration of a solution [19].

The assay was designed to examine the influence of these parameters on the tendency to precipitate carbonate, silicate and sulphate minerals within given ranges: 1) for temperatures between 15 °C and 30 °C and 2) for pressures from 10 bar to 20 bar. The sampling step for the temperature parameter was defined as 1 °C in a selected range of values, while for the transmembrane pressure parameter it was defined as 1 bar in the range from 10 bar to 20 bar. Additionally, research was also conducted using a transmembrane pressure value of 40 bar. The upper limit of the range set for the temperature parameter was adjusted to the fact that in industrial installations the desalination process of geothermal water was conducted at a temperature of 30 °C [21]. Following on from that, the lower limit of the range was determined on the basis of the possible temperature at which water can be directly introduced into the water treatment installation in order to make better use of the heating potential of geothermal water. This temperature was established as 15 °C. As far as the transmembrane pressure parameter was concerned, the ranges were adjusted to the values which are commonly used in the nanofiltration process (10 bar) and reverse osmosis (20 bar). Other desalination process parameters were constant.

### 2.3. Methodology of the laboratory tests

Apart from modelling research, laboratory tests were also conducted on the water treatment process. The SEPA CF-HP membrane
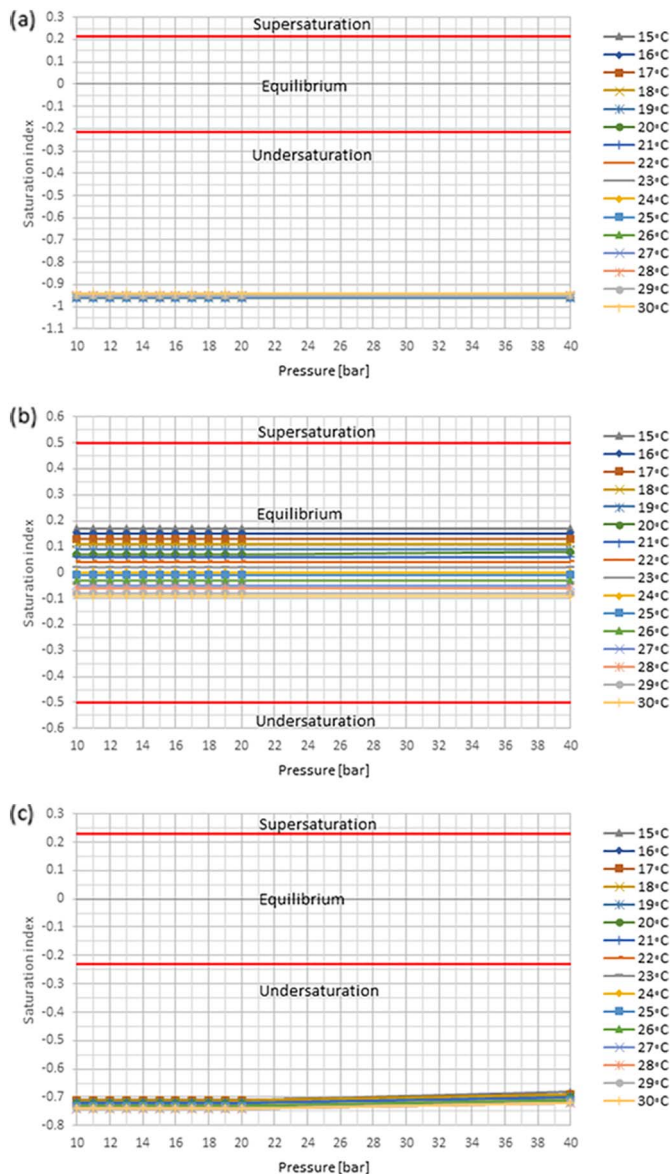
Fig. 3. The values of the Saturation Index for the (a) anhydrite, (b) barite and (c) gypsum solid phase in selected ranges of transmembrane pressure values (10–20 bar and 40 bar), including the value of water temperature (from 15 to 30 °C).
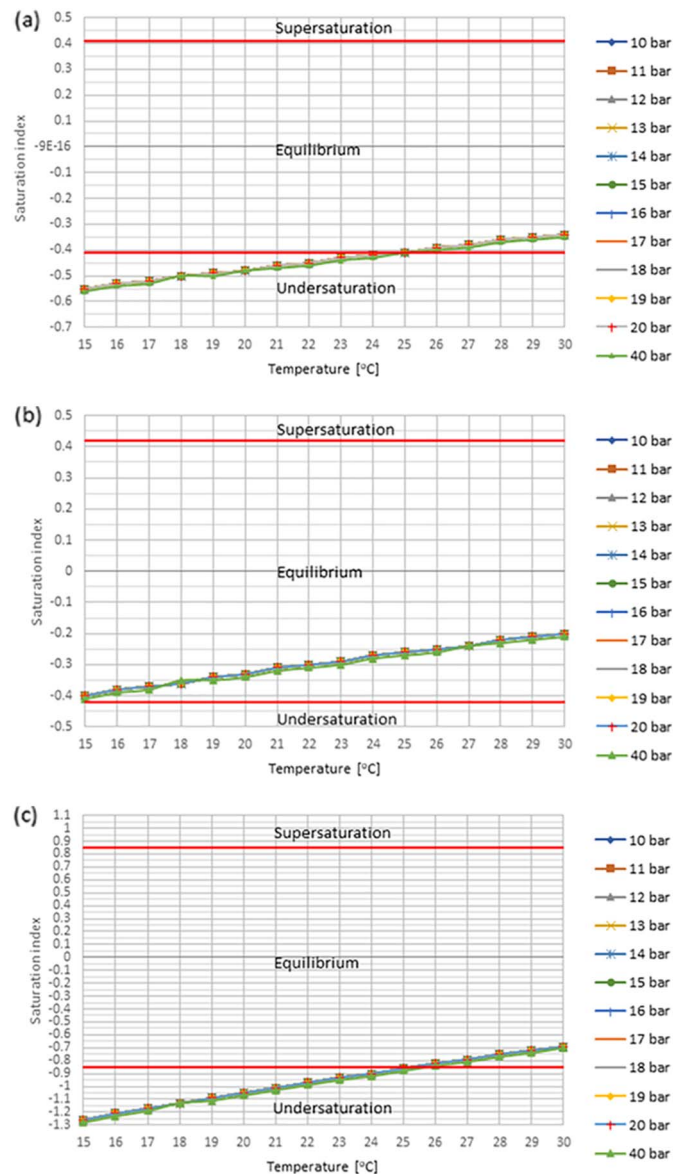


Fig. 4. The values of the Saturation index for the (a) aragonite, (b) calcite and (c) dolomite solid phase in a selected range of water temperatures (from 15 to 30 °C), including the value of transmembrane pressure.

module of the American company Osmonics Inc. was used in "cross-flow" mode. The module was equipped with a DOW FILMTEC NF270 membrane. The experiment was carried out at a specified pressure of 10 bar. The active area of the membrane was 155 cm$^2$. Before research, each new membrane was conditioned by the filtration of deionized water to stabilize the permeate flux. The performance of the desalination process was determined by measuring the changes in permeate flux $J_v$:

$$J_v = \frac{V}{F \cdot t}$$

where: V – volume of permeate (L), F – active area of the membrane (m$^2$), f – filtration time (s).

### 2.4. Methodology of the membrane scaling survey

The morphology and chemical composition of the mineral components of the materials precipitated on the membrane surface were identified at micro scale with the use of the electron scanning microscope (SEM). An FEI Qanta 250 FEG scanning microscope equipped with an additional chemical composition analysis system, EDS EDAX equipment, based on energy dispersion scattering was used to complete the analysis.

### 3. Results and discussion

The hydrogeochemical modelling was conducted within the chosen ranges of parameters specified and with the defined sampling step. The *SI* values for transmembrane pressure for carbonate minerals: aragonite, calcite and dolomite are shown in Fig. 1. Fig. 2 presents the result of the research for silicate minerals: chalcedony, quartz, silica-gel and amorphous SiO$_2$ and Fig. 3 – for sulphate minerals: anhydrite, barite and gypsum. On each chart the borders of the equilibrium state are represented by red lines.

In the entire predetermined range of transmembrane pressure (values from 10 to 20 bar), the Saturation Indices for the chosen carbonate (Fig. 1), silicate (Fig. 2) and sulphate minerals (Fig. 3) were stable and presented the same value. As far as carbonate minerals are concerned,
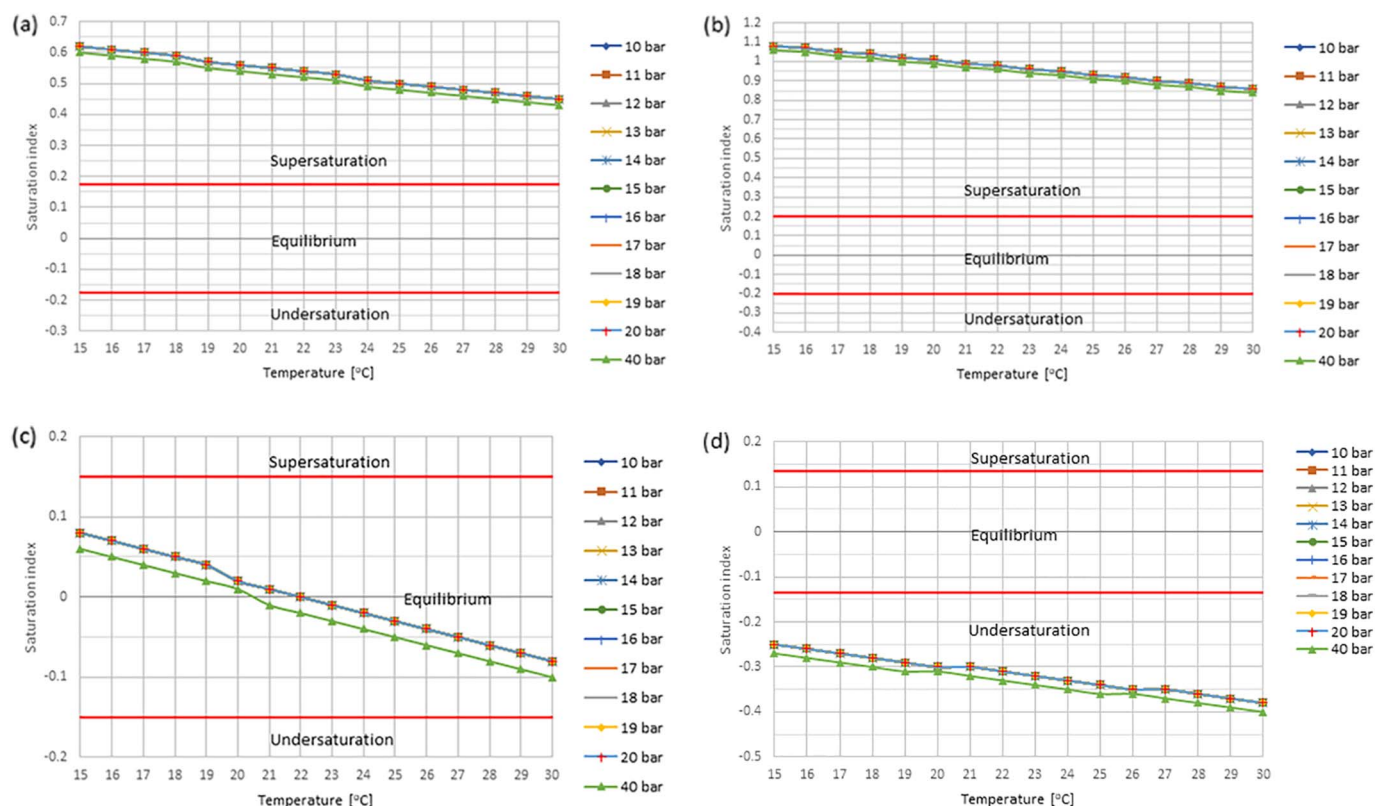
**Fig. 5.** The values of the Saturation Index for the (a) chalcedony, (b) quartz, (c) silica-gel and (d) amorphous SiO$_2$ solid phase in a selected range of water temperatures (from 15 to 30 °C), including the value of transmembrane pressure.

supersaturation of the solution was not found in all ranges of temperature and pressure analysed. The equilibrium state has been observed for calcite. For aragonite and dolomite with an increased temperature value of 25 °C, *SI* values also increase and the mineral forms are present from the undersaturated state to equilibrium. Chalcedony and quartz (SiO$_2$) present supersaturation of their solutions and a tendency to precipitate on the membrane surface in all the range of temperature analysed. Silica-gel presents a state of equilibrium, and amorphous SiO$_2$ is in an undersaturated state of solution (Fig. 2). In the case of sulphate minerals, only the equilibrium state was observed as far as barite is concerned. Others mineral forms analysed present undersaturation of solutions.

A number of research studies suggest that temperature and pH are important factors which have an influence on the precipitation of carbonate minerals [16,22–24]. Elevated concentrations of HCO$_3^-$ and Ca$^{2+}$, and especially elevated water temperature causes scale formation by calcium carbonate [25]. Calcium carbonate is reported to exist in six forms, three hydrated forms and three anhydrous crystalline polymorphic forms [16]. The calcium carbonate polymorphs are as follows in order of decreasing stability: calcite, aragonite, vaterite, monohydrocalcite, ikaite and amorphous calcium carbonate [26]. The process of crystallization of calcium carbonate is controlled by temperature, pH and the concentration of specific ions [16]. Aragonite, which is thermodynamically less stable, can occur in certain temperature conditions or in the presence of other ions. Burton and Walter [27] indicate that with increasing temperature, precipitation rates of aragonite and calcite increase, which corresponds with the results obtained. Anthony et al. [16] reported that the formation of silica scale is dependent on the pH of the silica concentration in solution. When the concentration of silica increases, soluble silica exhibits a tendency to polymerise and cause the scaling phenomenon, which is a common problem encountered in desalination processes due to low solubility and high concentrations of silicates in feed water

[28–29]. Moreover, it is assumed that the most common scale-forming constituents in membrane processes are, inter alia, CaSO$_4$ and BaSO$_4$. The basic condition necessary for scales to form is for these to exceed the solubility limit, i.e. the solubility product at thermodynamic equilibrium [30]. One of the major limitations arises from membrane fouling caused by different inorganic salts, which reduces permeate flux, increases feed pressure, decreases product quality, and ultimately shortens membrane life [31]. Transmembrane pressure is an important operating parameter in membrane filtration. It directly affects the permeate flux and is frequently used to control feed water recovery [32]. When the temperature increases, the maximum value for the flux increases as well. Consequently, an appropriate range for the working transmembrane pressure can be estimated to prevent any undesirable membrane fouling [33].

The influence of pressure on scale formation has been analysed by several researchers [34–35]. Bhandari et al. [34] analysed the effect of pressure on the nucleation kinetics of barite, anhydrite, and celestite. They concluded that the nucleation kinetics of these minerals are highly dependent on the hydrostatic pressure applied even under a constant thermodynamic driving force, that is, at the same level of supersaturation. But in further cases only high pressure can influence reaction kinetics. Reed and Palandri [35] attempted to separate the effects of changes of temperature, pressure, pH, salinity and redox state by varying only one at a time. They concluded that it is quite difficult to separate these variables, even in the context of contrived computer models. In the natural setting, simultaneous change in these variables, and many more especially those involving composition, must be the normal circumstance. As presented in Figs. 1–6 in cases of carbonate (aragonite and calcite) and all silicate minerals, an increase in the pressure value to 40 bar slightly decreases the *Saturation Index* for each mineral. A reverse relationship was reported with gypsum. Here a pressure increase to 40 bar increases the tendency to precipitate the mineral form analysed. In nature, at high temperatures
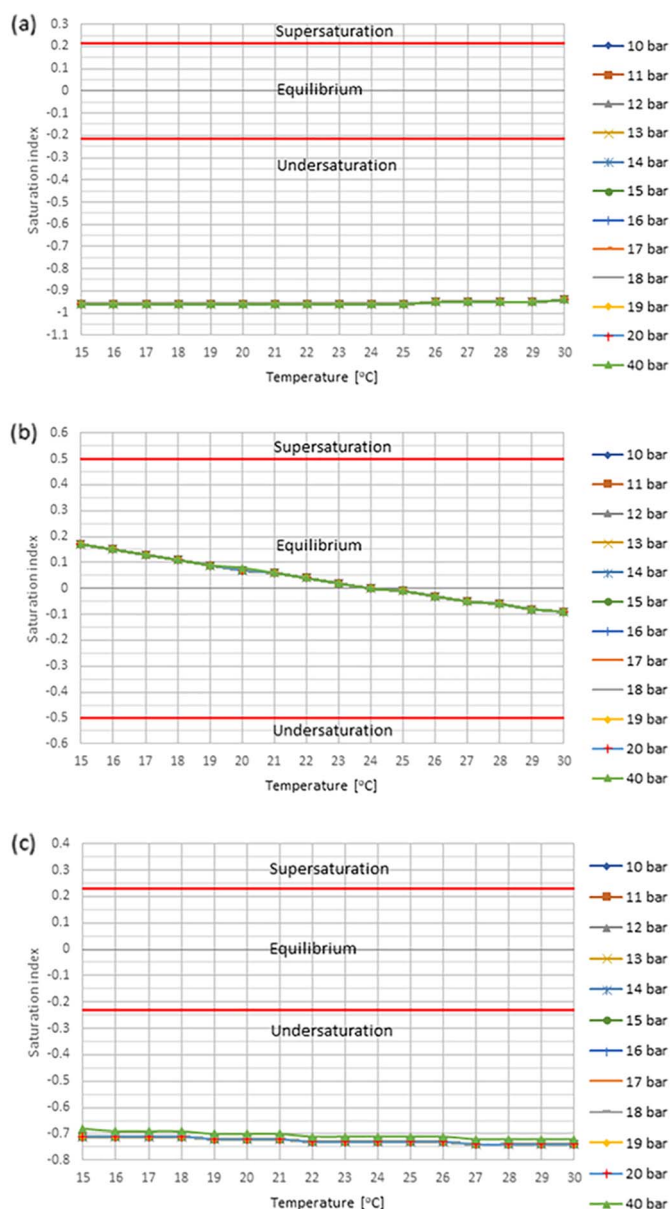
Fig. 6. The values of the Saturation index for the (a) anhydrite, (b) barite and (c) gypsum solid phase in a selected range of water temperatures (from 15 to 30 °C), including the value of transmembrane pressure.
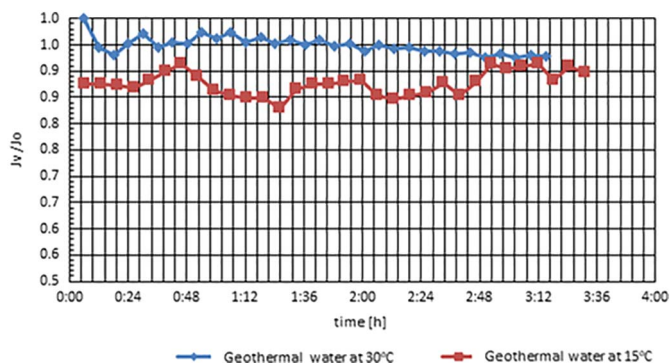


Fig. 7. The changes of relative permeate flux during in both nanofiltration processes conducted at a specific transmembrane pressure (10 bar).

and pressures, new crystals may grow in solid material and re-crystallization and formation of new minerals is also possible. So, in consequence, the prediction of a mineral's precipitation from water can change, depending on the parameters of the processes which we take into consideration. Also, one of the most important factors will be the possibility of undertaking modelling with access to a large mi-nerals database, presented for ex. by the Wateq 4f or phreeqC data bases. They include about 650 reactions and items of thermodynamic data, which is most important during geochemical modelling.

In our research, we concluded that in general, it can be stated that for silicate minerals, for an observed temperature increase of one degree, a decrease in *SI* value by about 1–4% is observed relative to the previous value (except for silica-gel for which the changes are considerably greater). A similar tendency was observed for carbonate minerals, where for an observed temperature increase of one degree, an increase in the *SI* value by about 1–8% is observed relative to the previous value. In view of the phenomenon of concentration polar-isation on the membrane [36] observed for the equilibrium state identified by geochemical modelling, precipitation of sediments may already occur when carrying out the process of nanofiltration/reverse osmosis. In the case of the geothermal water used in the study, ex-ceedance of $SI = 0 \pm 0.05$ log K for the carbonate forms examined and the occurrence of a risk of deposition of secondary minerals on the surface of the membrane may occur at a temperature of 25 °C for aragonite and dolomite and 15 °C for calcite. For the siliceous forms in turn, chalcedony and quartz exhibit a tendency to precipitate in the entire temperature spectrum from 15 to 30 °C while silica-gel exhibits a state of equilibrium in the temperature range considered, but the state of saturation of solution with this mineral form decreases at a temperature of approximately 21 °C. The amorphous form of $SiO_2$ should not constitute a threat to the membrane across the full tem-perature range. The sulphate minerals anhydrite and gypsum are in the undersaturated state in the entire spectrum from 15 to 30 °C, whereas barite exhibits a state of equilibrium in the entire tempera-ture range examined. The state of saturation of solution with the barite form decreases at a temperature of 24 °C. From the information given above, it follows that in the context of the results of geochemical modelling, to optimise the water treatment the process should be carried out at a temperature of about 15 °C. However, the level of transmembrane pressure will not have a significant effect on mem-brane scaling.

Nanofiltration tests carried out in the same modelled geothermal water in laboratory-scale conditions [37] at two different values of temperature: 15 and 30 °C and at a pressure of 10 bar shows the re-lationship with the modelling results. Fig. 7 shows changes in relative permeate flux with time. Generally, in both cases the process of water treatment proceeded in a stable manner. A slight decrease in permeate flux was observed especially in the case of geothermal water at a temperature of 30 °C. The membranes used in the laboratory tests were subjected to further analysis to identify the occurrence of mineral de-posits on their surface. Photomicrographs of the membranes obtained from a SEM are shown in Figs. 8 and 9.

Individual concentrations of different deposits are observed on the membrane surface. Based on the SEM images of the membranes, it can be concluded that the carbonate and sulphate minerals examined are untraceable on the membrane surface (Fig. 8). This result is consistent with the hydrogeochemical modelling which indicates that carbonate and sulphate minerals have no tendency to precipitate. On the other hand, some of the silicate minerals selected are traceable in the pho-tomicrograph images (Fig. 9). Siliceous sediments, identified on the membrane after carrying out tests at a temperature of 15 °C (Fig. 8), represent only about 5% of the sediments. There has also been a slight precipitation of calcite, which correlates with the results from hydro-geochemical modelling.
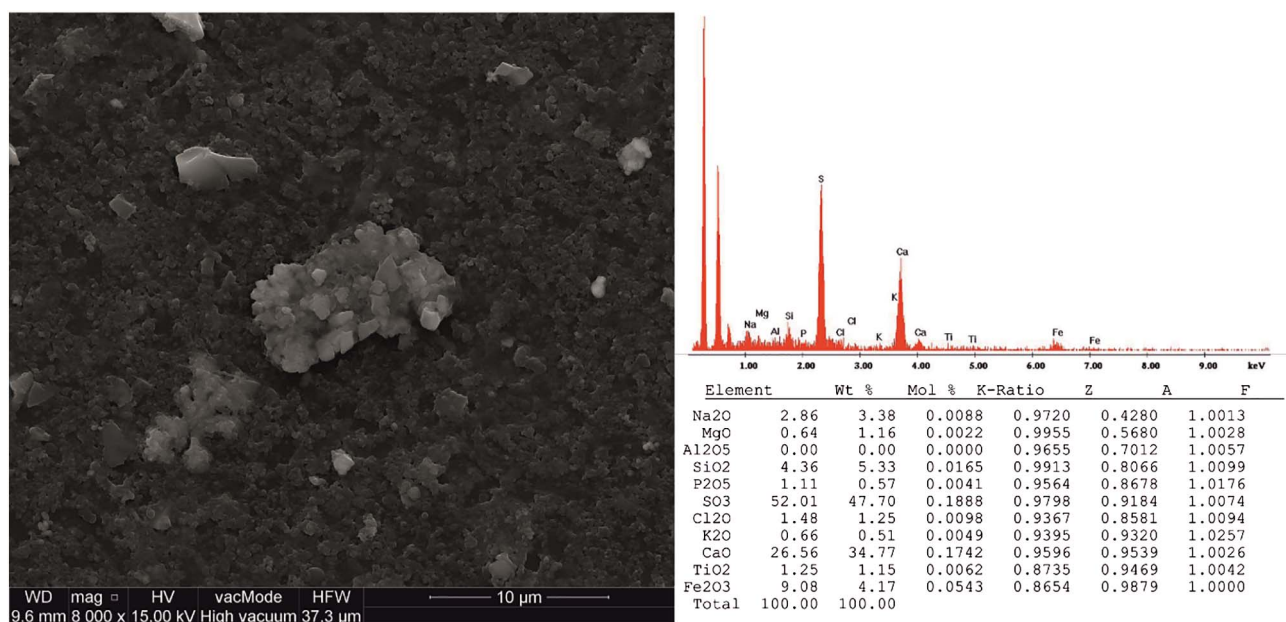
| Element | Wt % | Mol % | K-Ratio | Z | A | F |
|---|---|---|---|---|---|---|
| Na2O | 2.86 | 3.38 | 0.0088 | 0.9720 | 0.4280 | 1.0013 |
| MgO | 0.64 | 1.16 | 0.0022 | 0.9955 | 0.5680 | 1.0028 |
| Al2O5 | 0.00 | 0.00 | 0.0000 | 0.9655 | 0.7012 | 1.0057 |
| SiO2 | 4.36 | 5.33 | 0.0165 | 0.9913 | 0.8066 | 1.0099 |
| P2O5 | 1.11 | 0.57 | 0.0041 | 0.9564 | 0.8678 | 1.0176 |
| SO3 | 52.01 | 47.70 | 0.1888 | 0.9798 | 0.9184 | 1.0074 |
| Cl2O | 1.48 | 1.25 | 0.0098 | 0.9367 | 0.8581 | 1.0094 |
| K2O | 0.66 | 0.51 | 0.0049 | 0.9395 | 0.9320 | 1.0257 |
| CaO | 26.56 | 34.77 | 0.1742 | 0.9596 | 0.9539 | 1.0026 |
| TiO2 | 1.25 | 1.15 | 0.0062 | 0.8735 | 0.9469 | 1.0042 |
| Fe2O3 | 9.08 | 4.17 | 0.0543 | 0.8654 | 0.9879 | 1.0000 |
| Total | 100.00 | 100.00 | | | | |

**Fig. 8.** SEM-EDS images of the NF270 membrane surface in membrane autopsy after use in a membrane test at a temperature of 15 °C.



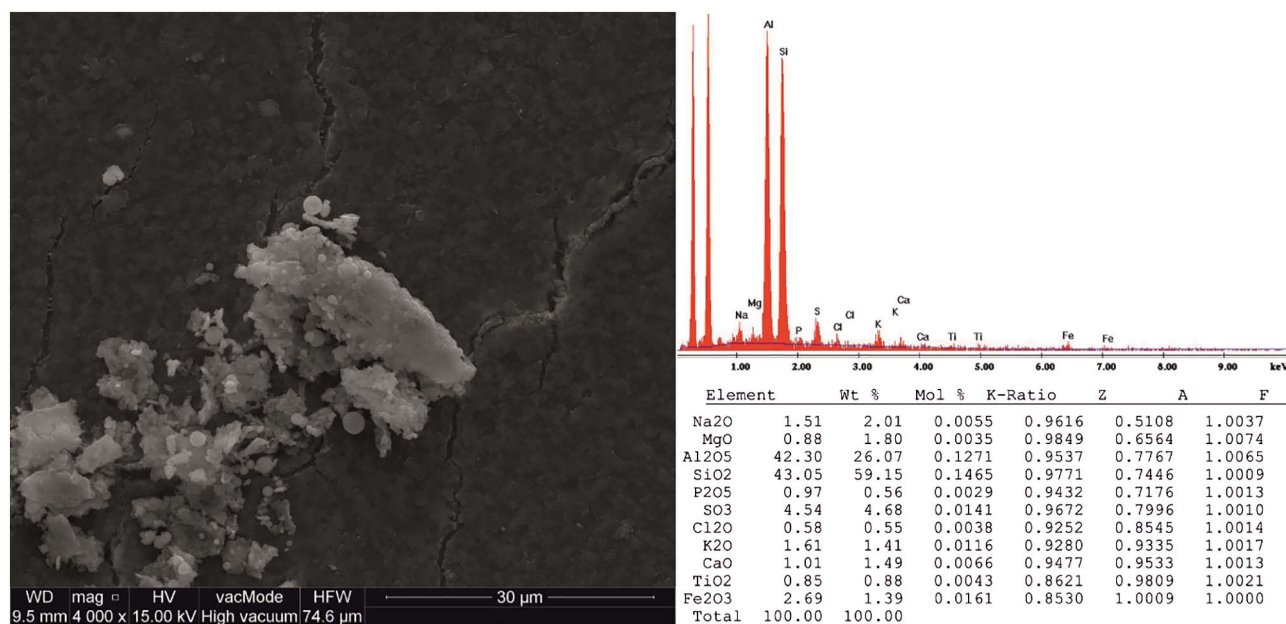| Element | Wt % | Mol % | K-Ratio | Z | A | F |
|---|---|---|---|---|---|---|
| Na2O | 1.51 | 2.01 | 0.0055 | 0.9616 | 0.5108 | 1.0037 |
| MgO | 0.88 | 1.80 | 0.0035 | 0.9849 | 0.6564 | 1.0074 |
| Al2O5 | 42.30 | 26.07 | 0.1271 | 0.9537 | 0.7767 | 1.0065 |
| SiO2 | 43.05 | 59.15 | 0.1465 | 0.9771 | 0.7446 | 1.0009 |
| P2O5 | 0.97 | 0.56 | 0.0029 | 0.9432 | 0.7176 | 1.0013 |
| SO3 | 4.54 | 4.68 | 0.0141 | 0.9672 | 0.7996 | 1.0010 |
| Cl2O | 0.58 | 0.55 | 0.0038 | 0.9252 | 0.8545 | 1.0014 |
| K2O | 1.61 | 1.41 | 0.0116 | 0.9280 | 0.9335 | 1.0017 |
| CaO | 1.01 | 1.49 | 0.0066 | 0.9477 | 0.9533 | 1.0013 |
| TiO2 | 0.85 | 0.88 | 0.0043 | 0.8621 | 0.9809 | 1.0021 |
| Fe2O3 | 2.69 | 1.39 | 0.0161 | 0.8530 | 1.0009 | 1.0000 |
| Total | 100.00 | 100.00 | | | | |

**Fig. 9.** SEM-EDS images of the NF270 membrane surface in membrane autopsy after use in a membrane test at a temperature of 30 °C.

## 4. Conclusions

The prediction of scaling during water treatment using a membrane is the most important initial consideration. There are many parameters which can have an influence on this phenomenon. Especially the physical (pH, temperature) and chemical composition of the water treated.

Our research showed, that the *Saturation Index* for the chosen carbonate, silicate and sulphate minerals have almost the same values of *SI* for the entire predetermined range of transmembrane pressure (10 to 20 bar) for each water temperature (from 15 to 30 °C). But in the case of the high transmembrane pressure value of 40 bar, a slight decrease in the *SI* values has been observed for selected carbonate and all silicate minerals. In contrast, for sulphate minerals, especially for gypsum, there is a tendency observed for the value of *SI* to increase slightly following the increased transmembrane pressure. The results of the

modelling study lead us to conclude that to optimise the water treatment process, it should be carried out at a temperature of about 15 °C. On the other hand, the volume of transmembrane pressure should not have a significant effect on the degree of membrane scaling.

The results of membrane analysis after water treatment tests showed that the same minerals have been found precipitated on the membrane surface, which was presented as the effect of hydrogeochemical modelling. Some of the silicate minerals selected for analysis were traceable in the images of photomicrographs of the membranes used obtained from an electron scanning microscope. Both chalcedony and quartz exhibit a tendency to precipitate which is also apparent in the SEM image of the membrane used. The studies conducted unambiguously show relationships between the hydrogeochemical modelling results and the results of real research obtained during tests. In this context, the PHREEQC program carried out with a rich database on mineral

formations (e.g. wateq4f, phreeqC base) and with the possibility of inputting the chemical composition of raw geothermal water, pH, the temperature of feed water and a specified transmembrane pressure value as input parameters, can be a useful tool with regard to applications related to the prognosis of scaling phenomena during the treatment of mineralised waters. Prediction of the occurrence of scaling phenomena and the selection of appropriate input parameters can increase the permeate flux value and reduce the cost of the desalination process by decreasing the scaling problem.

## Acknowledgements

## References

[1] D.L. Gallup, Treatment of geothermal waters for production of industrial, agricultural or drinking water, Geothermics 36 (2007) 473–483.
[2] V.G. Gude, Geothermal source potential for water desalination – current status and future perspective, Renew. Sust. Energ. Rev. 57 (2016) 1038–1065.
[3] M. Bonte, B.M. van Breukelen, P.J. Stuyfzand, Temperature-induced impacts on groundwater quality and arsenic mobility in anoxic aquifer sediments used for both drinking water and shallow geothermal energy production, Water Res. 47 (2013) 5088–5100.
[4] K.V. Reddy, N. Ghaffour, Overview of the cost of desalinated water and costing methodologies, Desalination 205 (2007) 340–353.
[5] S.T. Mitrouli, M. Kostoglou, A.J. Karabelas, Calcium carbonate scaling of desalination membranes: assessment of scaling parameters from dead-end filtration experiments, J. Membr. Sci. 510 (2016) 293–305.
[6] B. Tomaszewska, M. Bodzek, Desalination of geothermal waters using a hybrid UF-RO process. Part II: membrane scaling after pilot-scale tests, Desalination 319 (2013) 107–114.
[7] M. Finster, C. Clark, J. Schroeder, L. Martino, Geothermal produced fluids: characteristics, treatment technologies, and management options, Renew. Sust. Energ. Rev. 50 (2015) 952–966.
[8] D. Lawler, J. Kweon, Integrated Water Treatment: Softeniing and Ultrafiltration, Iwa Publishing, 2003.
[9] A.G. Pervov, Precipitation of calcium carbonate in reverse osmosis retentate flow by means of seeded techniques – a tool to increase recovery, Desalination 368 (2015) 140–151.
[10] C. Kaya, G. Sert, N. Kabay, M. Arda, M. Yüksel, Ö. Egemen, Pre-treatment with nanofiltration (NF) in seawater desalination—preliminary integrated membrane tests in Urla, Turkey, Desalination 369 (2015) 10–17.
[11] L. Llenas, G. Ribera, X. Martinez-Llado, M. Rovira, J. de Pablo, Selection of nanofiltration membranes as pretreatment for scaling prevention in SWRO using real seawater, Desalin. Water Treat. 36 (2011) 310–318.
[12] M. Bodzek, A. Konieczny, A. Kwiecińska, Application of membrane processes in drinking water treatment – state of art, Desalin. Water Treat. 35 (1–3) (2011) 164–184.
[13] N. Hilal, H. Al-Zoubi, N.A. Darwish, A.W. Mohammad, M. Abu Arabi, A comprehensive review of nanofiltration membranes: treatment, pretreatment, modelling, and atomic force microscopy, Desalination 170 (2004) 281–308.
[14] B. Tomaszewska, M. Rajca, E. Kmiecik, M. Bodzek, W. Bujakowski, K. Wątor, M. Tyszer, The influence of selected factors on the effectiveness of pre-treatment geothermal water during nanofiltration process, Desalination 406 (2017) 74–82.
[15] T. Akin, A. Guney, H. Kargi, Modeling of calcite scaling and estimation of gas breakout depth in a geothermal well by using PHREEQC, Proceedings, Fortieth Workshop on Geothermal Reservoir Engineering Stanford University, Stanford,

California, 2011 January 26–28 2015, SGP-TR-204.
[16] A. Anthony, J. How Low, S. Gray, A.E. Childress, P. Le-Clech, G. Lesile, Scale formation and control in high pressure membrane water treatment systems: a review, J. Membr. Sci. 383 (1–2) (2011) 1–16.
[17] M. Karime, S. Bouguecha, B. Hamrouni, RO membrane autopsy of Zarzis brackish water desalination plant, Desalination 220 (2008) 258–266.
[18] V.A. Prisyazhniuk, Prognosticating scale-forming properties of water, Appl. Therm. Eng. 27 (2007) 1637–1641.
[19] D.L. Parkhurst, C.A.J. Appelo, Description of input and examples for PHREEQC version 3 – a computer program for speciation, batch-reaction, one-dimension transport and inverse geochemical calculations, U.S Geological Survey, Denver, Colorado, 2013.
[20] W. Ball James, Nordstrom D. Kirk, User's manual for wateq4f, with revised thermodynamic database and test cases for calculating speciation of major, trace, and redox elements in natural waters, US Geology Survey, 1991, pp. 91–183 (Open File Report).
[21] B. Tomaszewska, M. Bodzek, Desalination of geothermal waters using a hybrid UF-RO process. Part I: boron. Removal in pilot-scale tests, Desalination 319 (2013) 99–106.
[22] C. Tzotzi, T. Pahiadaki, S.G. Yiantsios, A.J. Karabelas, N. Andritsos, A study of $CaCO_3$ scale formation and inhibition in RO and NF membrane processes, J. Membr. Sci. 296 (2007) 171–184.
[23] L.F. Greenlee, F. Testa, D.F. Lawler, B.D. Freeman, P. Moulin, The effect of anti-scalant addition on calcium carbonate precipitation for a simplified synthetic brackish water reverse osmosis concentrate, Water Res. 44 (2010) 2957–2969.
[24] Z. Li, R.V. Linares, S. Bucs, C. Aubry, N. Ghaffour, J.S. Vrouwenvelder, Calcium carbonate scaling in seawater desalination by ammonia–carbon dioxide forward osmosis: mechanism and implications, J. Membr. Sci. 481 (2015) 36–43.
[25] R. Menzri, S. Ghizellaoui, M. Tlili, Calcium carbonate inhibition by green inhibitors: thiamine and pyridoxine, Desalination 404 (2017) 147–154.
[26] S.S. Salek, O.D. Bozkur, A.G. van Turnhout, R. Kleerebezem, M.C.M. van Loosdrecht, Kinetics of $CaCO_3$ precipitation in an anaerobic digestion process integrated with silicate minerals, Ecol. Eng. 86 (2016) 105–112.
[27] E.A. Burton, L.M. Walter, Relative precipitation rates of aragonite and Mg calcite from seawater: Temperature and carbonate ion control, Geology 15 (1987) 111–114.
[28] E.A. Rashed, M.M. Elshafei, M.A. Hiekl, M.E. Matta, K.M. Naguib, On-line dosing of ammonium biflouride for reduction of silica scaling on RO membranes, HBRC J. 12 (2) (2016) 205–211.
[29] G. Braun, W. Hater, C. Zum Kolk, C. Dupoiron, T. Harrer, T. Götz, Investigations of silica scaling on reverse osmosis membranes, Desalination 250 (2010) 982–984.
[30] P. Schausberger, G.M. Mustafa, G. Leslie, A. Friedl, Scaling prediction based on thermodynamic equilibrium calculation — scopes and limitations, Desalination 244 (2009) 31–47.
[31] S. Shirazi, Lin Che-Jen, D. Chen, Inorganic fouling of pressure-driven membrane processes, Desalination 250 (2010) 236–248.
[32] Lin Che-Jen, P. Rao, S. Shirazi, Effect of operating parameters on permeate flux decline caused by cake formation – a model study, Desalination 171 (2004) 95–105.
[33] C.L. Astudillo-Castro, Limiting flux and critical transmembrane pressure determination using an exponential model: the effect of concentration factor, temperature, and cross-flow velocity during casein micelle concentration by microfiltration, Ind. Eng. Chem. Res. 54 (2015) 414–425.
[34] N. Bhandari, A.T. Kan, F. Zhang, Z. Dai, F. Yan, G. Ruan, Z. Zhang, Y. Liu, R. van Eldik, M.B. Tomson, Mineral precipitation kinetics: assessing the effect of hydrostatic pressure and its implication on the nucleation mechanism, Cryst. Growth Des. 16 (9) (2016) 4846–4854.
[35] M.H. Reed, J. Palandri, Sulfide mineral precipitation from hydrothermal fluids, Rev. Mineral. Geochem. 61 (2006) 609–631.
[36] M. Bodzek, K. Konieczny, Membrane techniques in the removal of inorganic anionic micropollutants from water environment state of the art, Arch. Environ. Protect. 37 (2) (2011) 15–29.
[37] M. Rajca, M. Bodzek, B. Tomaszewska, M. Tyszer, E. Kmiecik, K. Wątor, Prevention of scaling during desalination of geothermal water by means of nanofiltration, Desalin. Water Treat. 73 (2017) 198–207.